JOURNAL OF MATERIALS SCIENCE 10 (1975) 2075–2081

Precipitation in an Al-1.78 wt % Hf alloy after rapid solidification

NILS RYUM
Institutt for Fysikalsk Metallurgi, N.T.H., Trondheim, Norway

A metallographic study has been made of an Al–1.78 wt % Hf alloy after rapid solidification, and after high temperature annealing of the as-cast alloy. After solidification, Hf stays in supersaturated solid solution with a rather inhomogeneous distribution. On annealing, spheres and dendrites of an intermediate Al_3Hf phase with $L1_2$ structure, and perfectly coherent with the matrix, are formed. The spheres form by a continuous, the dendrite by a discontinuous precipitation reaction. After continued annealing the $L1_2$ structure is replaced by a laminated structure of $L1_2$ and $D0_{22}$, where $D0_{22}$ is the equilibrium structure of Al_3Hf. The precipitation reactions in the systems Al–Hf and Al–Zr are compared.

1. Introduction

Metastable alloys may be obtained by rapid solidification [1]. The characterization of these types of alloys has recently received much attention. An extensive reference list is given by Giessen in his survey [1]. The most interesting features of these alloys are the extension of the range of solid solubility, appearance of metastable phases as well as of amorphous-like structures.

On subsequent annealing after solidifaction, the supersaturated alloy is likely to decompose by reactions similar to those taking place during ageing of precipitation-hardening alloys. These decomposition reactions have been less extensively studied. Results obtained by X-ray techniques and microhardness indicate that the supersaturated solid solution may be quite stable [1–3]. The decomposition reactions in Al–Mn and Al–Zr have been studied in detail by electron microscopy [4–7].

In Al–Mn alloys, the properties of technological importance are probably connected with supersaturation of Mn after solidification and subsequent "heterogenization" during subsequent annealing [8]. The interest in the Al–Zr alloy is due to the pronounced affect of small amounts of Zr (~1.0 to 1.5 wt %) on the recrystallization properties and subgrain structure in Al alloys [9]. This effect is due to the easy nucleation in the Al matrix of an intermediate cubic phase, Al_3Zr, which is coherent, finely dispersed, and has a high thermal stability. The discrepancies between the results obtained by Izumi and Oelschlägel [6] and Ryum [5] are discussed below.

The present investigation is part of a study of the structures and properties in aluminium transition-metal alloys after rapid solidification and annealing. The comparison between Al–Hf and Al–Zr is particularly interesting, because of the similarity between these two alloying elements.

The Al-rich part of the Al–Hf system has been studied by Rath *et al.* [10]. Their equilibrium diagram is shown in Fig. 1. The diagram is similar to that for Al–Zr as given by Fink and Willey [11]. The maximum solubility of Hf in Al (0.182 at.%) is, however substantially higher than the solubility of Zr in Al, which is only 0.085 at.%. Al_3Hf exists in two different crystallographic forms [12]: $D0_{23}$, which is believed to be a high-temperature form, isomorphous with the Al_3Ti, is tetragonal with $a = 3.899$ Å, $c = 17.155$ Å; and $D0_{22}$, believed to be a low temperature form, isomorphous with Al_3Zr, is also tetragonal with $a = 3.893$ Å, $c = 8.925$ Å.

2. Experimental

The alloy was prepared from 99.995% Al and an Al–10 wt % Hf master alloy obtained from Kawecki

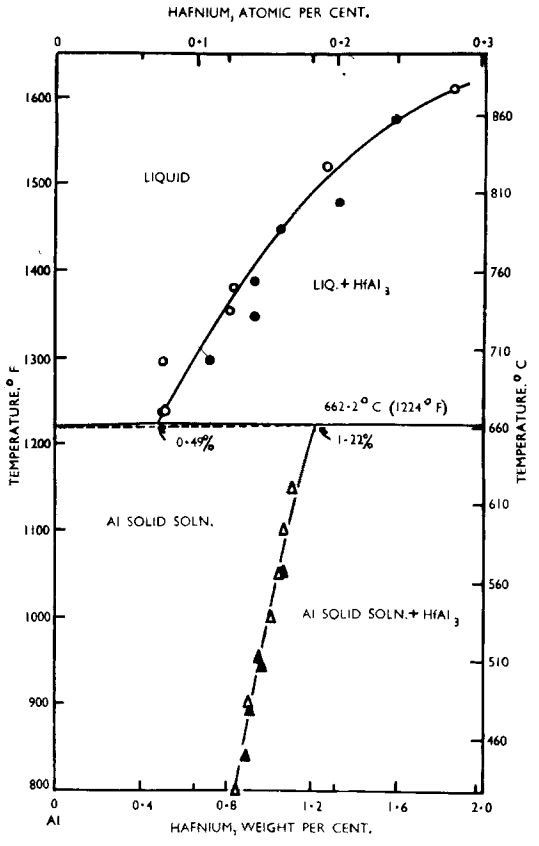

Figure 1 Aluminium end of the aluminium–hafnium equilibrium diagram. After Rath *et al.* [10].

Ltd. The melting and casting technique was the same as that used earlier for the Al–Zr alloy [5]. The Hf + Zr content, determined gravimetrically by cupferron, was 1.83 wt %. The impurities, determined by the mass absorption technique were Fe 0.03%, Si 0.01%, Mn 0.001%, Ti 0.007%, Cr 0.002%, Zn 0.001% and Zr 0.05%. Specimens, about 0.1 mm thick, were sliced from the cylindrical 12 mm diameter casting by means of spark-cutting. They were annealed in a salt bath furnace at temperatures ranging from 200 to 550° C for times ranging from few minutes to about 100 days. After annealing, the specimens were polished in a CH_5OH–$HClO_4$ electrolyte and inspected in the light microscope using Nomarksi phase contrast equipment. Thin foils were prepared by the window method using the same electrolyte, and inspected in a JEM 7 microscope.

3. Results

The as-cast structure as revealed in the light microscope is shown in Fig. 2. It is very similar to the one found in Al–Zr [5]. Particles formed during solidification were found throughout the matrix and on grain boundaries. X-ray microanalysis showed them to be rich in Fe and poor in Hf, but they were too small for a detailed quantitative analysis. Only after the longest annealing times at temperatures above 400° C could very small and heterogeneously distributed precipitates be observed in the light microscope.

The precipitation process was consequently followed in greater detail in the electron micro-

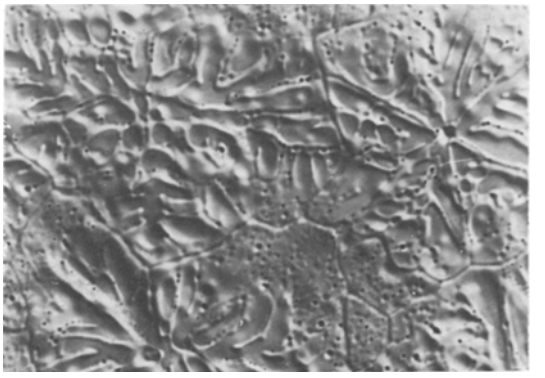

Figure 2 The as-cast structure, Nomarksi-phase contrast ×165.

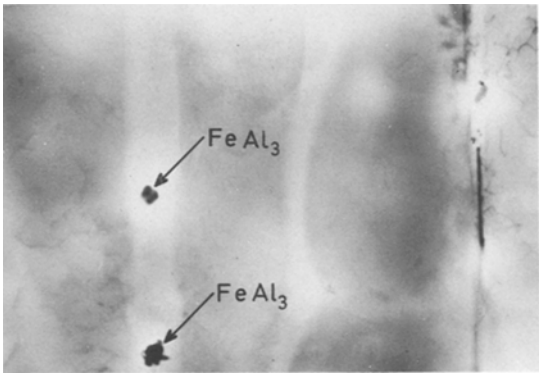

Figure 3 The as-cast structure, at low magnification in the electron microscope, ×5800.

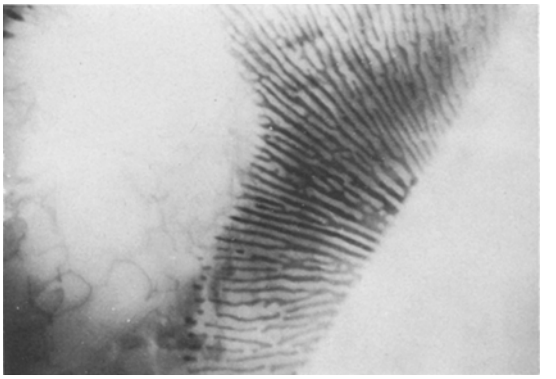

Figure 4 Discontinuously formed precipitates after 20 h at 200° C, ×13 000.

scope. The as-cast structure as revealed in the electron microscope at low magnification is shown in Fig. 3. The Hf-rich regions are visible as darker regions. The contrast is probably due to differences in thickness of the foil, caused by different polishing rates in Hf-rich and Hf-poor regions. In the Hf-poor regions nearly spherical particles, ~ 1–$2\,\mu m$ in diameter, were often seen. Elongated particles were also found on the grainboundaries. Electron diffraction analysis of the particles indicated them to be $FeAl_3$. On annealing at 200° C precipitates were found only in connection with grain boundaries. These were obviously formed by discontinuous precipitation (Fig. 4). Precipitates were not found in the matrix after the longest annealing times used at this temperature, 29 h. At 450° C, precipitates appeared rapidly in the matrix: these were usually gathered in clusters. After a relatively short annealing time, about 50 h, the precipitates were either spherical or they showed a dendritic appearance. The latter type was invariably found adjacent to grain boundaries; Fig. 5 shows the two types. The grain boundary, which is in poor contrast in this case, is indicated by an arrow. Occasionally, the spherical and dendritic precipitates were present in the same cluster (Fig. 6). Diffraction experiments showed both types of precipitate to have the same structure (Fig, 7a).

The pattern can be indexed according to the ordered cubic $AuCu_3$ structure (Ll_2), with $a_{Al_3Hf} = a_{Al}$ (Fig. 7b). The precipitates are thus very similar to those found in the Al–Zr alloy. In the Al–Zr system, rod-shaped precipitates were present instead of the dendritic type. Both the spheres and the rods were found to be surrounded by a strain

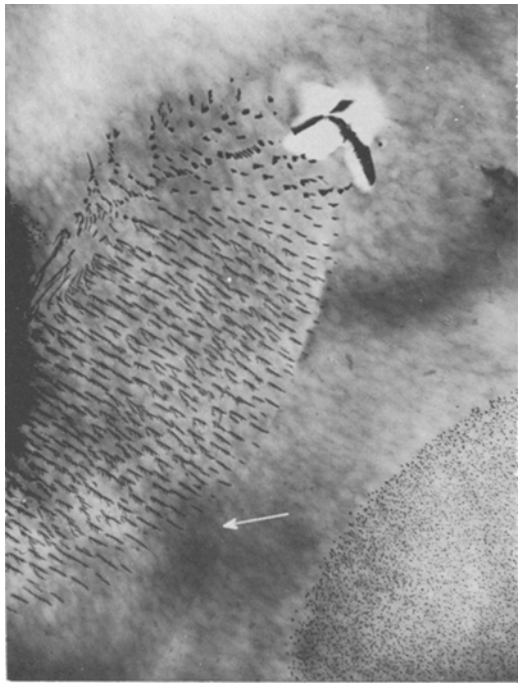

Figure 5 Spherical and dendritic type precipitates after annealing at 450° C for 100 h. Arrow indicates high-angle grain boundary, ×6000.

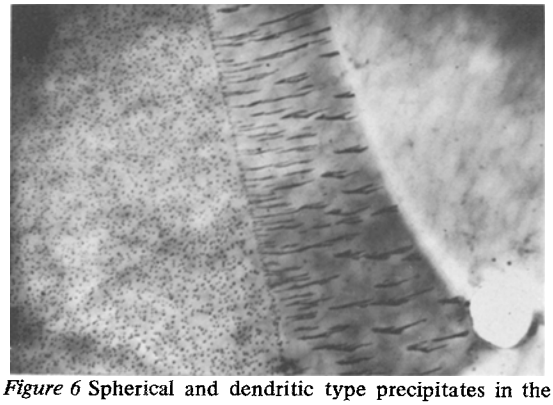

Figure 6 Spherical and dendritic type precipitates in the same cluster, ×13 000.

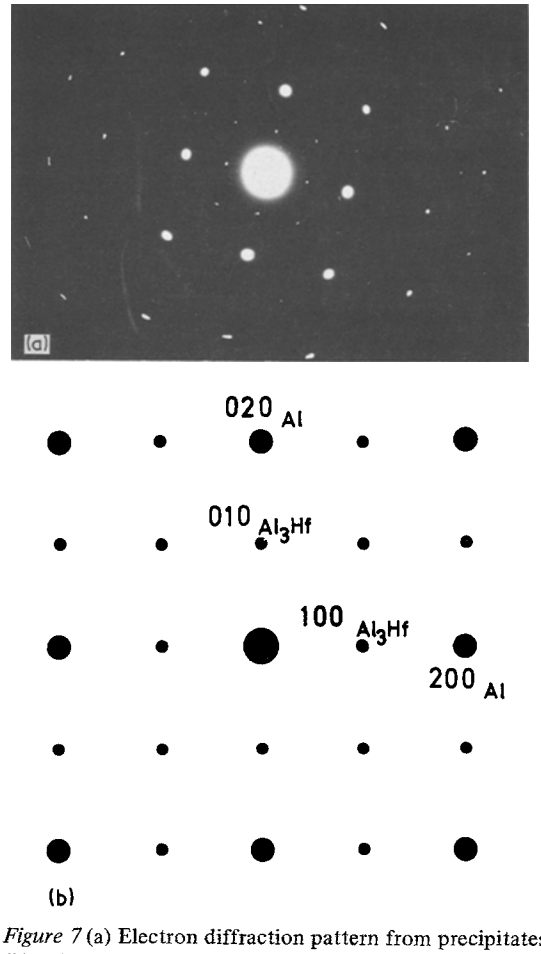

Figure 7 (a) Electron diffraction pattern from precipitates. (b) The pattern indexed according to the cubic (Ll_2) Al_3Hf structure.

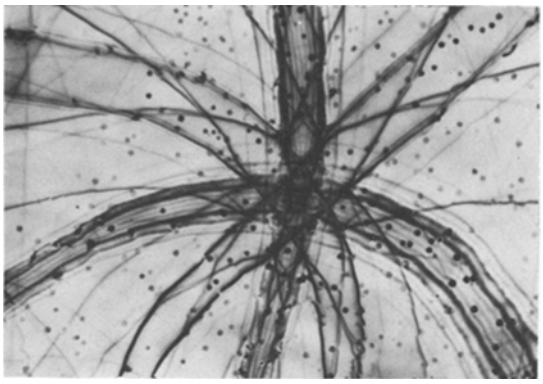

Figure 8 Micrograph showing no strain field present around the precipitates. (1 0 0) zone, ×13 000.

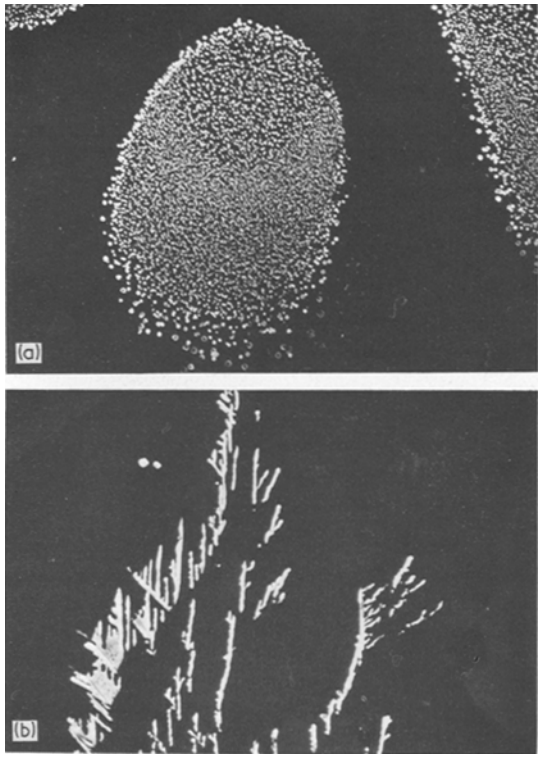

Figure 9 Annealed at 450° C for 70 days. The precipitates have changed only slightly. Dark-field with (1 0 0) Al_3Hf reflection. (a) ×5800, (b) ×10 000.

field [5]. In the present alloy, no strain field existed, as shown in Fig. 8. This state of precipitation changed only very slowly on prolonged annealing. The spheres in the periphery of the clusters appeared to coarsen more rapidly than those in the central area. An increasing departure from the spherical shape with increasing size was observed. Even after 70 days at 450° C many clusters contained a large number of spheres 100 to 300 Å in diameter. The dendritic precipitates were also very stable over long annealing times. Spheres and dendritic precipitates present after 70 days are shown in Fig. 9a and b. These are dark-field micrographs taken with a superlattice $(1\,0\,0)_{Al_3Hf}$ diffraction spot.

In some regions rod- and plate-shaped precipitates appeared after about 50 h with their long dimension in the ⟨1 0 0⟩ directions. Fig. 10a and b shows these types of precipitate, together with spheres which have become irregular in shape. The surface of the rod-shaped precipitates is also very irregular. In some of the precipitates a laminated structure developed with markings in the ⟨1 0 0⟩ direction as indicated by the arrow in Fig. 10b.

The diffraction pattern from this type of precipitate after relatively short and longer annealing times is shown in Fig. 11a and b. After a short annealing time, very long streaks with indistinct maxima pass through the Al_3Hf reflections in the ⟨1 0 0⟩ direction perpendicular to the long dimension of the precipitate. The indistinct maxima sharpen to diffraction spots and the intensity of the streaks decreases with increasing annealing time. The diffraction pattern obtained after the longest annealing time may be indexed according to a superposition of the equilibrium tetragonal,

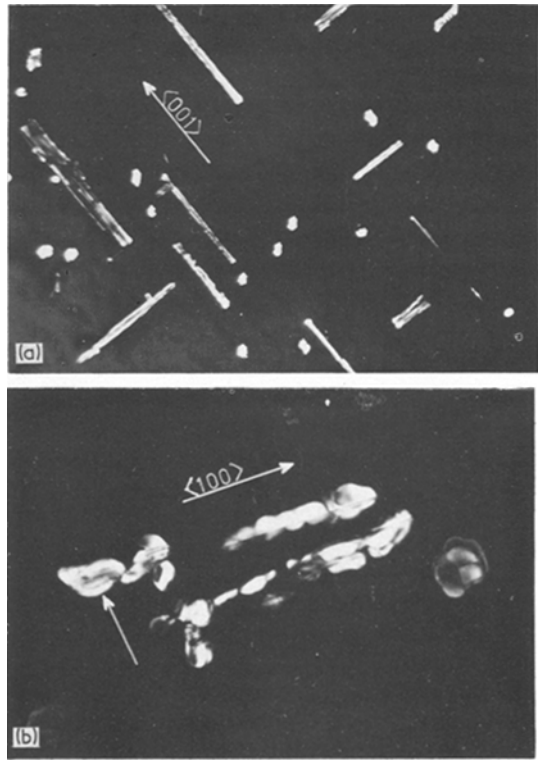

Figure 10 Plates and distorted spheres. (1 0 0) zone. (a) ×10 000, (b) ×60 000.

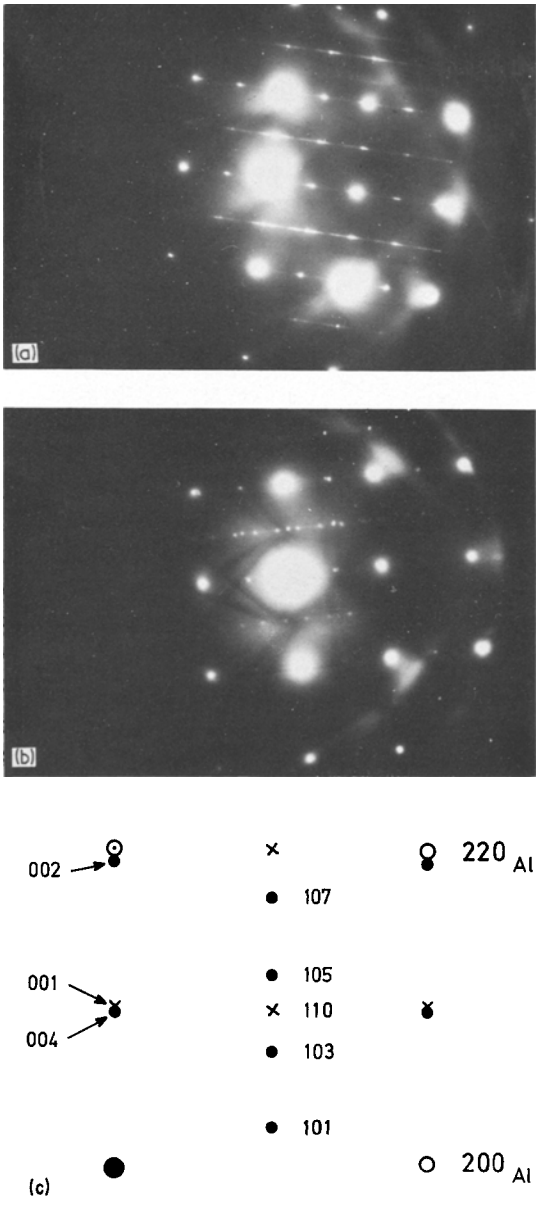

Figure 11 Diffraction pattern from plate-shaped precipitates: (a) 450° C for 50 days, (b) 450° C for 100 days, (c) indexing of (b) according to a mixture of cubic (Ll_2) and tetragonal ($D0_{22}$) Al_3Hf. X: reflections from the cubic Al_3Hf, •: reflections from the tetragonal Al_3Hf.

($D0_{23}$) and the intermediate cubic (Ll_2) Al_3Hf structures, as shown in Fig. 11c. The lattice parameters of the tetragonal structure were determined to be: $a = 4.05$ Å, $c = 16.9$ Å with $a_{Al} = 4.05$ Å as standard. When annealing at 550° C, the precipitates were nearly all of the dendritic type. The precipitates arranged in the ⟨1 0 0⟩ directions were present after ~ 5 h, but the equilibrium phase did not form even after 24 h at this temperature.

4. Discussion and conclusion

No Hf-rich precipitates were found in the as-cast condition in this alloy. This demonstrates the great tendency for Hf to remain in supersaturated solid solution after rapid solidification. The cellular as-cast structure (Fig. 2) indicates an inhomogeneous distribution of Hf. This was verified both in the X-ray micro-analyser and also by electron microscopic observations of an inhomogeneous distribution of precipitates after annealing. The cellular as-cast structure is common for many aluminium transition metal alloys [8].

Decomposition of the supersaturated solid solution on annealing occurs by the formation of an intermediate cubic Al_3Hf phase. This is completely coherent with the aluminium lattice, and no coherency strains could be observed in the electron microscope.

The different shapes of this intermediate phase, i.e. spherical and dendritic, clearly reflect the way in which they are formed. Spherical precipitates, which always occur in large clusters within the grains, are clearly formed by a continuous precipitation reaction taking place in regions with high Hf content. Dendritic precipitates are always associated with a grain boundary and are formed by a discontinuous precipitation reaction. At 200° C only the discontinuous reaction was observed. This probably indicates that the diffusion of Hf in Al is very slow, so that the precipitation takes place at a measurable rate only in a discontinuous manner in which the Hf atoms diffuse in a grain boundary region. The coarsening of the spherical and dendritic precipitates occurs very slowly. This also supports a low interfacial energy between the precipitates and the matrix and a low rate of diffusion of Hf in Al.

The reason why the spherical particles change shape when growing is not clear. A similar effect is observed in the Ni–Al alloys [13, 14]. When they are small (~300 Å), the coherent Ni_3Al precipitates are spherical, but they become cubic as they grow. In this case the change in shape is attributed to the presence of coherency strain around the precipitates [13]. This explanation is not valid for Al–Hf, since no coherency strain is present. In fact, Ni_3Al precipitates in Ni–Cr–Al alloys which have no coherency strain, remain spherical at all sizes [13].

The observations made on the Al–Hf alloy show great similarity with those made earlier on an Al–Zr alloy [5–7]. The spherical and rod-shaped

precipitates found in that system are most likely formed by the same reactions as the spheres and dendrites in the present alloy, i.e. by continuous and discontinuous precipitation respectively. In Al–Zr, the misfit between the intermediate cubic Al_3Zr phase and the matrix induced coherency strains around precipitates of both shapes, and also restricted the branching of the precipitates formed by discontinuous precipitation. Rod-shaped, and not dendritic, precipitates are thus found in that system. The suggestion made by Izumi and Oelschlägel [6, 7] that the rod-shaped precipitates form by strain-affected coarsening of spherical particles appears not to be probable.

The $D0_{22}$ structure may be formed by a shear movement $\mathbf{b} = \frac{1}{2}\langle 1\,1\,0\rangle$, on every other (1 0 0) plane in the Ll_2 structure (Fig. 12). (To obtain the correct $D0_{22}$-Al_3Hf structure, slight movements of the Hf and Al atoms out of the (1 0 0) planes are also necessary, see Imuzi and Oelschlägel [6]). This amounts to the introduction of antiphase boundaries in a regular manner in the Ll_2 structure. By the faults in the stacking of the antiphase boundaries, thin slabs of imperfect $D0_{22}$-Al_3Hf structures are obtained inserted in the Ll_2-Al_3Hf structure. This transformation is apparently responsible for the formation of the rod- and plate-shaped precipitates formed after long annealing times, and explains the long streaks, and the appearance of reflections from both these structures from the same precipitate (Fig. 11a and b) and also the laminated appearance (Fig. 10).

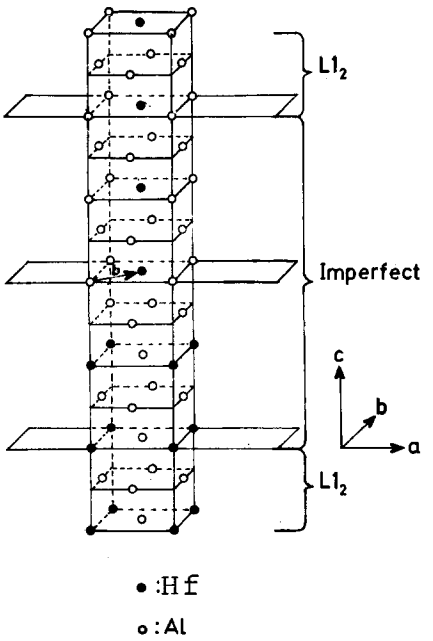

Figure 12 The relation between the Ll_2 and $D0_{22}$ structures. By a shear movement on every other (0 0 1) plane a distance $\frac{1}{2}\langle 1\,1\,0\rangle$ the Ll_2 is transformed to the $D0_{22}$ structure. By a shear movement on only one (0 0 1) plane produces an imperfect unit cell of the $D0_{22}$ structure.

The decomposition of the supersaturated solid solution may thus be represented schematically in the following way:

$$\text{solid solution} \rightarrow \left\{\begin{array}{l}\text{spheres (cont.precip.)}\\ \text{dendrites (discont.precip.)}\\ Ll_2 \text{ structure}\end{array}\right\} \rightarrow \left\{\begin{array}{l}\text{and plates, rods, laminated structures of } Ll_2 \text{ and } D0_{22}\\ \downarrow\\ D0_{22}\end{array}\right\}$$

The transition $Ll_2 + D0_{22}$ (imperfect) $\rightarrow D0_{22}$ (perfect) which involves the stacking of the antiphase boundaries in the right sequence, is a very sluggish reaction and the pure equilibrium phase $D0_{22}$-Al_3Hf was not observed.

Acknowledgements

Thanks are due to ÅSV, Norway, for making the mass absorption analysis of the alloy used for this investigation. This work was carried out at Sentralinstitutt for Industriell Forskning, Oslo and supported by grants from Norges Teknisk-Naturvitenskapelige Forskningråd (NTNF) (The Royal Norwegian Council for Scientific and Industrial Research) and A/S Årdal og Sunndal Verk. Thanks are due to my colleagues at Sentralinstituttet and to Dr Jon Gjønnes at the University of Oslo for their interest in this work and for many helpful discussions. Thanks are also due to siv.ing. J.H. Søvik who kindly assisted me during the final preparation of the manuscript.

References

1. B. C. GIESSEN, ed. "Developments in the Structure Chemistry of Alloy Phases", (Plenum Press, New York, 1969) p. 227.
2. G. FALKENHAGEN and W. HOFMANN, *Z. Metallk.* **43** (1951) 69.
3. N. I. VARIC, L. M. BUROV and K. E. KOLESNICENKO, *Fiz. Metal. Metalloved* **15** (1963) 292.
4. O. IZUMI, D. OELSCHLÄGEL and A. NAGATA, *Trans. JIM* **2** (1968) 227.
5. N. RYUM, *Acta Met.* **17** (1969) 292.
6. O. IZUMI and D. OELSCHLÄGEL, *Z. Metallk.* **60** (1969) 845.
7. *Idem, Scripta Met.* **3** (1969) 619.
8. D. ALTENPOHL, "Aluminium and Aluminiumlegierungen" (Springer Verlag, Berlin, 1965).
9. N. RYUM, *J. Inst. Metals* **94** (1966) 191.

10. B. R. RATH, G. P. MOHANTRY and L. F. MONDOLFO, *J. Inst. Metals* **89** (1960/61) 248.
11. W. L. FINK and L. A. WILLEY, *Trans. Met. Soc. AIME* **133** (1939) 69.
12. W. B. PEARSON, "Lattice Spacings and Structure of Metals and Alloys", Vol. 1/11 (Pergamon Press).
13. A. J. ARDELL and R. B. NICHOLSON, *Acta Met.* **14** (1966) 1295.
14. E. HORNBOGEN and M. ROTH, *Z. Metallk.* **58** (1967) 842.

Received 30 April and accepted 20 May 1975.